Journal of Marine Science and Technology

Volume 24 | Issue 3 Article 4

SLOPE STABILITY ANALYSIS OF TRANSIENT SEEPAGE UNDER EXTREME CLIMATES: CASE STUDY OF TYPHOON NARI IN 2001

Chia-Feng Hsu
Department of Harbor and River Engineering, National Taiwan Ocean University, Keelung, Taiwan , R.O.C.,
chiafeng1013@gmail.com

Lien-Kwei Chien
Department of Harbor and River Engineering, National Taiwan Ocean University, Keelung, Taiwan , R.O.C.

Journal of Marine Science and Technology, Vol. 24, No. 3, pp. 399-412 (2016)
DOI: 10.6119/JMST-015-0813-1

SLOPE STABILITY ANALYSIS OF TRANSIENT SEEPAGE UNDER EXTREME CLIMATES: CASE STUDY OF TYPHOON NARI IN 2001

Chia-Feng Hsu and Lien-Kwei Chien

Key words: extreme climate, finite-element analysis, transient seepage, slope stability analysis, permeability, factor of safety (FS).

ABSTRACT

The effects of climate change, the inherent fragility of geological structures in Taiwan, and questionable developmental practices have led to the occurrence of numerous slope disasters, most of which were triggered by the extreme rainfall associated with typhoons. Therefore, this study collected rainfall data associated with typhoons striking northern Taiwan over the last 17 years, as a follow up to estimating database of extreme rainfall events. Most previous investigations regarding the impact of storms on slope stability focused on solutions with conditions, such as static groundwater levels or steady pore pressure. Previous studies have used software STABL to analyze slope stability but failed to consider the influence of groundwater seepage or changes in pore pressure during rainfall events. Thus, we proposed an improved method of defining a partitioning rainfall to select the most representative rainfall events, whereupon a comprehensive overview of the associated rainfall patterns was constructed using finite-element analytical software SEEP/W. We simulated the transient seepage of unsaturated soils and input the results into SLOPE/W to conduct slope stability analysis. A comparison of STABL results demonstrates that the outcomes of this study are more applicable to real-world cases than existing methods for the evaluation of slope stability.

I. INTRODUCTION

Taiwan largely comprises steep terrain with a fragile geological structure. As a result, heavy seasonal rainfall tends to produce rock falls, landslides, and debris flows, resulting in the loss of lives and property.

Slope failure often occurs following a storm, which leads to the conclusion that slope failure is related to rainfall. In fact, this connection has been confirmed in numerous studies. The influence of rainfall on landslides varies considerably according to landslide dimensions, kinematics, material involved, etc. Most shallow failures are triggered by short intense storms (Lumb, 1975; Brand et al., 1984; Cannon and Ellen, 1985; Wieczorek, 1987; Guzzetti et al., 1992; Morgan et al., 1997; Crosta, 1998; Corominas and Moya, 1999; Flentje et al., 2000; Paronuzzi et al., 2002), while most deep-seated landslides are affected by long-term variations in annual rainfall over a period of several years (Bonnard and Noverraz, 2001).

Two types of landslide-triggering rainfall thresholds can be established (Aleotti, 2004): (i) Empirical thresholds based on historic analysis of rainfall/landslide occurrences (i.e. statistical) (Campbell, 1975; Caine, 1980; Crozier and Glade, 1999); (ii) Physical thresholds based on numerical models that take into account the relationship between rainfall, pore pressure, and slope stability by coupling hydrologic and stability models (Montgomery and Dietrich, 1994; Wilson and Wieczorek, 1995; Crosta, 1998; Terlien, 1998).

After confirming the connection between rainfall and slope failure, numerous researchers focused on determining when rain is likely to reach slope failure thresholds. In Southern California, rainfall exceeding 140% of the normal amount (meaning the average of recorded data from the last hundred years) is considered sufficient to trigger slope failure mechanisms (Slosson, 1969; Slosson and Krohn, 1982). Wilson (1993) suggested that the rainfall threshold for slope instability in San Francisco is 125% of the normal amount. Wieczorek (1987) derived the same result in San Francisco. Brand et al. (1984) came to the following conclusions: (a) More than half of the slope failures in Hong Kong were caused by rainfall; and (b) rainfall intensity of 70 mm/hr is the critical threshold beyond which slope failure is likely to occur. Considering the connection between rainfall and slope failure, it would be reasonable to expect that preventive measures to deal with the above-mentioned risk factors should minimize losses due to landslides.

Nonetheless, rainfall and the infiltration processes leading to slope failure vary with time and location. Factors that influence infiltration such as the intensity, duration, and patterns of rainfall as well as hydrological conditions are numerous and

Paper submitted 04/16/15; revised 06/26/15; accepted 08/13/15. Author for correspondence: Chia-Feng Hsu (e-mail: chiafeng1013@gmail.com).
Department of Harbor and River Engineering, National Taiwan Ocean University, Keelung, Taiwan , R.O.C.

highly complex, which makes it hard to adopt an analytic method based purely on theory. Therefore, we sought to resolve this problem using numerical simulation. The simulation of rainfall proved highly effective in elucidating how hydrological conditions, such as groundwater flow and pore-water pressure, change over time.

Chang et al. (2004) used the finite element software program SEEP/W to analyze the stability of unsaturated soil slopes. They postulated that the infiltration of rainwater affects the dissipation of negative pore-water pressure in slopes as well as the stability of unsaturated soil slopes. However, in the event that the soil mass has an adequate capacity of water storage and the saturated hydraulic conductivity is small, then the time required for negative pore-water pressure to dissipate may be greater than the duration of rainfall at the surface, even if the infiltration rate is longer than or equal to the hydraulic conductivity of saturated soil. In this case, the infiltration of rainwater exerts little influence on the stability of slopes comprising unsaturated soil.

Lui (2004) used the finite element program SEEP/W to simulate slope infiltration behavior associated with four types of unsaturated soil: uniform sand, sandy loam, silty clay and Longtan laterite. Their results revealed that slope infiltration behavior in unsaturated soil is affected by the permeability of the soil. The high permeability coefficient of unsaturated soil accelerates the infiltration speed, which expands the area influenced by it. Most previous investigations regarding the impact of storms on slope stability focused on solutions with conditions, such as static groundwater levels or fixed pore pressure.

Dahal et al. (2009) dealt with the parameters contributing to rainfall-triggered landslides that occurred during an extreme monsoon rainfall event on 23 July 2002, in the south-western hills of Kathmandu valley, in the Lesser Himalaya, Nepal. Landslide modeling was performed using SEEP/W and SLOPE/W to understand the relationship between pore-water pressure variations in soil layers and spatial variations in landslide occurrence. The main contributing factors associated with slope failures in the region included soil characteristics, low angle of internal friction of fines in soil, medium range soil permeability, the presence of clay minerals in soil, bedrock hydrogeology, and human intervention.

Lee et al. (2009) presented a simple model for the preliminary evaluation of rainfall-induced slope failure. Their results revealed that the ratio of rainfall intensity to soil saturated permeability plays an important role in determining critical rainfall patterns. They employed the suction envelope (representing the worst suction distribution in soil) to compute the factor of safety for soil slopes using the modified infinite-slope-limit-equilibrium method. The PERISI model was developed based on the findings of numerical simulation. The suction envelope and factor of safety computed using the PERISI model are in good agreement with the results obtained from SEEP/W and SLOPE/W computer programs as well as the results derived from the model developed by Rahardjo et al. in 1995.

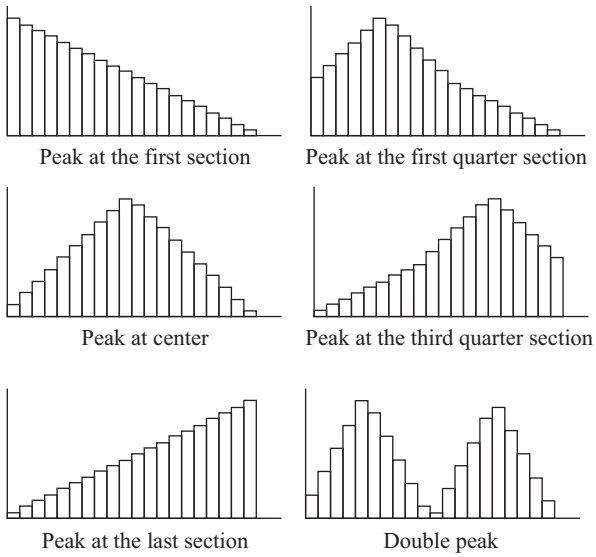

Fig. 1. The six common rainfall patterns in Taiwan (Shih, 2001).

As shown above, studies conducted over the last decade in which SEEP/W was paired with SLOPE/W for the analysis of dam foundation seepage and slope stability produced results with a high degree of reliability. In contrast, analysis of slope stability using STABL fails to consider the influence of groundwater seepage or changes in pore-water pressure during rainfall events. The approach proposed in this study involves the integration of extreme rainfall distribution with numerical simulation related to rainfall seepage. This approach is able to present a acceptably accurate indication of seepage behavior in the study area in real time as well as its influence on slope stability. The evaluation of vulnerable slopes must be conducted with extreme caution in every stage of development (before, during, and after). This study focused on slope stability analysis prior to the development of hillsides. It is hoped that our findings will provide a valuable reference for the selection of locations suitable for development.

II. METHODOLOGY

1. Pattern Analysis of Typhoon-Induced Rainfall

According to the Central Weather Bureau, most of the typhoons that hit Taiwan occur between May and November. August usually accounts for 30% of the total as well as many of the strongest events. Rainfall associated with typhoons can cover an enormous area, lasting for days.

1) Rainfall Patterns

A rainfall hydrograph is a rain chart for a specific period, usually shown in the form of a histogram, also known as a rainfall hyetograph or rainfall pattern. Rainfall patterns change with meteorological conditions. For example, seasonal rains differs from torrential rains caused by a typhoon, such that the rainfall patterns are different. There are six common rainfall patterns in Taiwan, as shown in Fig. 1: first point (peak in the

Table 1. Rain-field division method (Lee, 2006).

Type	Various definitions of 'continuous rain'
I	No rain within 24 consecutive hours before the rain started and after the rain ended.
II	No rain within 12 consecutive hours before the rain started and after the rain ended.
III	Take the point at which hourly precipitation > 4 mm as the starting point of effective rainfall; take the point in which hourly precipitation < 4 mm for 3 consecutive hours as the end point of the effective rainfall. The span between the start point and the end point is considered continuous rain.
IV	Take the point at which 24-hr accumulated precipitation reaches 10 mm as the starting point of effective rainfall; take the starting point of the rainfall in which 24-hr accumulated precipitation < 10 mm as the end point of the effective rainfall. The span between the start point and the end point is considered continuous rain.
V	Take the point in which hourly precipitation > 4 mm as the starting point of effective rainfall; take the point in which hourly precipitation < 4 mm for 6 consecutive hours as the end point of effective rainfall. The span between the start point and the end point is considered continuous rain.
VI	Take the point in which 12-hr accumulated precipitation reaches 10 mm as the starting point of effective rainfall; take the starting point of rainfall in which the 12-hr accumulated precipitation < 10 mm as the end point of effective rainfall. The span between the start point and the end point is considered continuous rain.

first section), 1/4 point (peak in the first quarter section), 2/4 point (peak in the center), 3/4 point (peak in the third quarter section), final point (peak in the last section), and double point (double peak) (Shih, 2001).

2) Rainfall Intervals

A suitable interval must be selected to facilitate the sorting of rainfall data. The Central Weather Bureau uses the following 16 intervals: 5, 10, 20, 30, 40, 60, 80, 90, 100 minutes and 2, 3, 4, 6, 12, 18, 24 hours. The yearly maximum rainfall intensity data recorded by rainfall gauge stations of the Water Resources Agency and Taiwan Power Company are classified into the following 13 intervals: 5, 10, 20, 30, 40, 60, 80, 90, 100 minutes and 2, 3, 4, 6, 12, 18, 24 hours. This study focuses on typhoons that strike northern Taiwan, which are characterized by rainfall of long duration; therefore, we selected hourly intervals.

3) Selection of Rain-Field Division Method

This study focused on the precipitation data of typhoons in particular, disregarding storms of short duration. Determining which rainfall data to select depends on the way that rainfall patterns are divided to derive accumulated rainfall, rainfall duration, and rainfall intensity. A number of previous studies dealing with methods for the division of rain-fields are described in the following:

(1) Shih (2001) used 90% of total precipitation (issued by Central Weather Bureau) as the reference precipitation, and duration that reaches this particular reference precipitation is considered the duration of the typhoons.
(2) Chang (1995) took continuity, timing, duration, and the total precipitation of rainfall into account, dividing long duration rainfall events into two-hour sections.
(3) Lee (2006) integrated rain-field divisions suggested by the various methods proposed in previous studies, and then sorted these into 6 types, as shown in Table 1.

The six types of rain-field divisions show the following: Types I, II and IV are of longer durations, produce larger accumulated rainfall, and exhibit lower average rainfall intensity; Type III is of a shorter duration, produces less accumulated rainfall, and exhibits higher average rainfall intensity; Types V and VI are of longer rainfall duration and produce accumulated precipitation within a reasonable range (Lee, 2006). So we used the rainfall patterns of Types V and VI to simulate typhoons that hit northern Taiwan. For the sake of objectivity, we try to use the derived average value from these two patterns as the reference rainfall intensity for seepage analysis.

2. Study Area

1) Location of Study Area

The research area is located in Xindian City, a satellite city of the Taipei metropolitan area, in the south area of the Taipei Basin. Xindian City covers 120 square kilometers of land, of which 12.2% is a plains region and the remainder is hillsides lying south to north. Except for the plains region in the north part of the city, this area comprises hillsides with slope of 30% or higher.

2) Integration of Typhoon Rainfall Patterns

The CKS Bridge Station is the rainfall station closest to the study area. This study integrated 17 years of data related to typhoons that struck northern Taiwan between 1996 and 2012, with a focus on those followed a westbound typhoon routes 1 to 5. According to rainfall data from the CKS Bridge Station, a total of 37 typhoons struck the area during the study period.

Field tests conducted on the Joffre alluvial gravel terraces in the upper reaches of Lan-Yang River by Hsu et al. (2000) showed that in terms of rainfall events and infiltration, rainfall intensity of less than 4.85 mm/hr and total rainfall of less than 21 mm would be insufficient to affect soil less than 60 cm deep. Among the 37 typhoons in this study, two typhoons (Utor in 2001 and Morakot in 2003) produced rainfall less than the minimum threshold at the CKS Bridge rainfall Station (rainfall intensity failed to reach 4 mm/hr). Thus, we excluded these events from the study. Figs. 2 and 3 and Table 2 show the rainfall patterns for Typhoon Nari in 2001.

3. Brief Summary

A review of rain-field division methods illustrated their

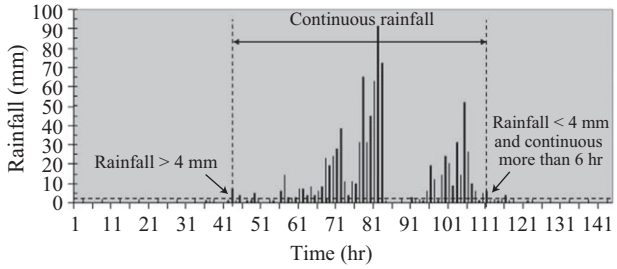

Fig. 2. Rainfall diagram of Typhoon Nari in 2001: rainfall threshold of 4 mm-6 hr.

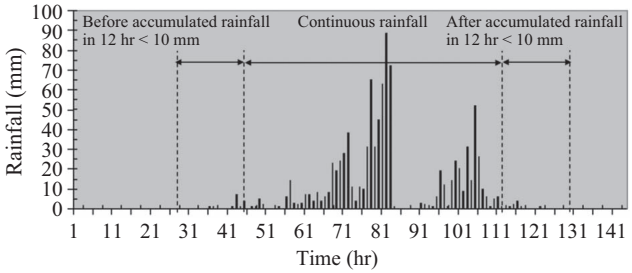

Fig. 3. Rainfall diagram of Typhoon Nari in 2001: rainfall threshold of 10 mm-12 hr.

Table 2. Rainfall patterns of typhoon Nari in 2001.

Type / Condition	Rainfall threshold of 4 mm-6 hr	Rainfall threshold of 10 mm-12 hr	Average
Rainfall pattern	peak at center	peak at center	peak at center
Total rainfall	923 mm	916 mm	920 mm
Rainfall duration	69 hr	68 hr	69 hr
Rainfall intensity	13.4 mm/hr	13.5 mm/hr	13.5 mm/hr

Table 3. Rain-field divisions associated with 35 typhoons.

Item	Total rainfall (mm)	Rainfall duration (hr)	Rainfall intensity (mm/hr)	Note
Total Average value	162	31	7	
Maximum in one field	920	69	13.5	Typhoon Nari (2001)
Maximum in an hour	91	1	91	Typhoon Nari (2001)

Note: Rainfall patterns following the peak in the third quarter which accounted for 31.25% of the rainfall.

considerable influence over rainfall parameter calculation. This study used Ming-Hsi Lee's (2006) analysis as a reference, in which (1) continuous rain with 4 mm-6 hr rainfall threshold and (2) continuous rain with 10 mm-12 hr accumulated rainfall threshold are used to estimate the expected duration and accumulation of rainfall within a set range. Using rainfall data from the CKS Bridge Station from 1996 to 2012 (including 35 typhoons), we obtained average values from the two analysis methods. The total average value, maximum in one field, and maximum in one hour are presented in Table 3.

In the Study of Flood Control and Sediment Management Due to Climate Change of Tamsui River (1/2), the Water Resources Planning Institute (WRPI) of the Water Resources Agency (2012) defined extreme rainfall as "typhoon events with the most severe disasters in Taipei City and simulations of the recorded highest rainfall." In terms of practical operations, this would mean considering one of the greatest typhoon events in the history of Northern Taiwan, Typhoon Nari. Our study area is also situated at the edge of the Taipei Basin. The extreme rainfall results of this study are consistent with those obtained by the WRPI, thereby indirectly verifying the reliability of the rain-field division model proposed in this study.

Thus, this study used the above rain-field division results as infiltration boundary conditions in the software program SEEP/W.

4. Numerical Simulation

Rainfall and infiltration processes vary with time and location. Factors that influence infiltration, such as the intensity, duration, and patterns of rainfall as well as critical hydrological conditions are numerous and complex. This makes it nearly impossible to use purely theoretical analysis to investigate the process of slope infiltration. Numerical simulation of rainfall can be used to elucidate how hydrological conditions, such as groundwater flow and pore-water pressure, change over time.

1) Seepage Analysis

SEEP/W is finite-element CAD software used for the analysis of groundwater seepage and excess pore-water pressure dissipation within porous materials such as soil and rock. Comprehensive formulation allows users to deal with a range of problems, from simple saturated steady-state problems to sophisticated saturated/unsaturated time-dependent problems.

SEEP/W is able to model saturated as well as unsaturated flow, which greatly broadens the range of problems that can be analyzed. In addition to traditional analysis on steady-state saturated flow, the saturated/unsaturated formulation of SEEP/W makes it possible to analyze seepage as a function of time and consider processes such as the infiltration of precipitation.

2) Slope Stability Analysis

Using limit equilibrium, SLOPE/W is able to model variable slope pore-water pressure conditions under a wide range of soil conditions, such as heterogeneous, complex stratigraphy, and slip surface geometry. It also uses a variety of methods to analyze geotechnical engineering problems, including slip surface deformation, pore-water pressure conditions, soil properties, and various loading methods.

Thus, this study adopted the SEEP/W subprogram of GeoStudio to simulate the infiltration behavior of transient seepage in natural slopes under the influence of typhoon-induced rainfall. We then analyzed the influence of changes in ground-water

level and pore-water pressure on slope stability. Using SEEP/W, we examined the infiltration and seepage of rainwater into slopes to derive the relationship between pore-water pressure and time in saturated and unsaturated soils. The features of the SLOPE/W subprogram were then utilized to conduct slope stability analysis using the limit equilibrium method.

III. NUMERICAL ANALYSIS OF THE STUDY AREA

The research area is a proposed development project in Taipei County, covering a total area of 76.23 hectares. The project is divided into three phases, the first and second of which have already been completed. We selected the undeveloped region located in the northeastern part of the study area as the area for simulation. Its geological structure is similar to the areas in the first and second phases of development, and its natural slope conditions are suitable for pre-development slope stability analysis.

1. Stratigraphic Distribution

The study area is located in the foothills of western Taiwan. Outcrop and drilling data revealed that nearby hills are composed of the Miocene, i.e., a Nanchuang layer and a gravel layer. A thick layer of massive sandstone makes up most of the layers.

2. Stratigraphic Distribution and Engineering Properties of the Area

The area of construction and development is divided into two principal areas: the northwestern area and the southeastern area. Ten holes (DH-1 to DH-10) were drilled in these areas.

3. Stability Analysis of Natural Slope at Area of Research Operations

An examination of the existing topography and stratigraphic distribution at the research area determined that the failure mode in the clay-gravel layer, weathered rock layer, and overburdened layer in the shape of an arc would be linear.

GEOSTUDIO 2004 was used to perform slope stability analysis. We considered the slope steepness over the entire area as well as the thickness of the overburden layer, the position of the dip slope, and other factors. For subsequent simulations, we selected three sections in which slope failure was most likely to occur (Fig. 4).

1) Soil Status under Normal (non-typhoon) Conditions

The soil was found to maintain its natural moisture content under normal circumstances and ground water levels were also maintained at their normal levels. The soil parameters as calculated by a contracted engineering consultant are presented in Table 4 (Chang, 2004).

Different analytical methods to specify sliding surfaces produce very different results. To facilitate further comparisons, we applied the function "Auto Locate" to the following SLOPE/W simulations. The results are presented in Fig. 5. The safety

Table 4. Average soil parameters at research area.

Soil parameters	γ_t (kN/m^3)	γ_{sat} (kN/m^3)	c' (kPa)	φ' (°)	note
First layer of L1-L1	19.6	19.6	9.8	30	Backfill layer
Second layer of L1-L1	23.5	23.5	117.7	32	weak weathered to fresh bedrock
First layer of L2-L2	19.6	19.6	9.8	30	Overburden layer
Second layer of L2-L2	23.5	23.5	117.7	32	weak weathered to fresh bedrock
First layer of L3-L3	20.6	20.6	9.8	35	Laterite gravel
Second layer of L3-L3	23.5	23.5	29.4	30	Moderate to highly weathered rock

Source: Chang (2004).

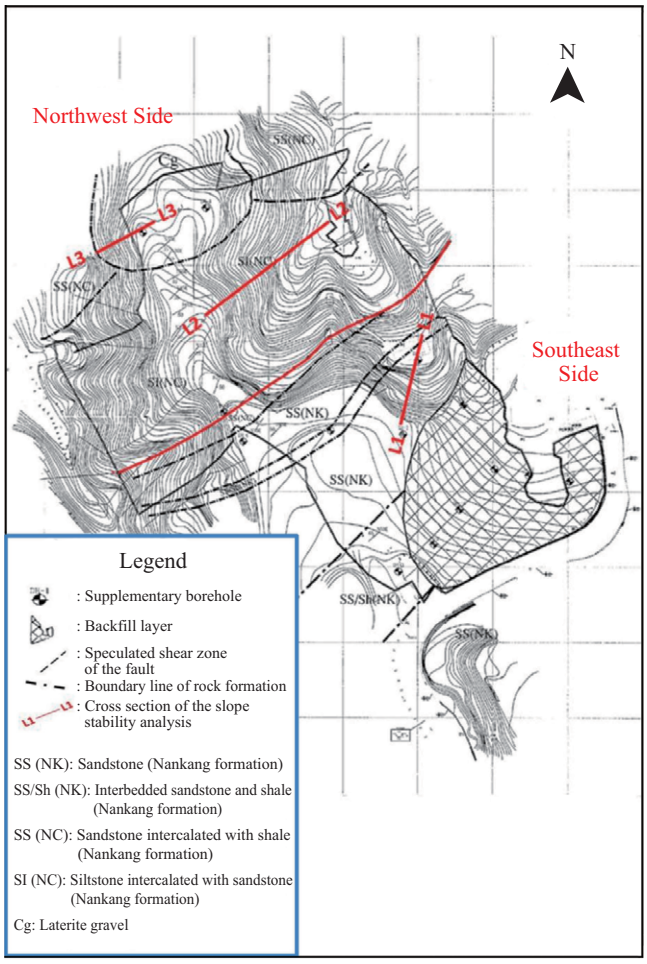

Fig. 4. Section location of geological map used in slope stability analysis (Scale: 1/500).

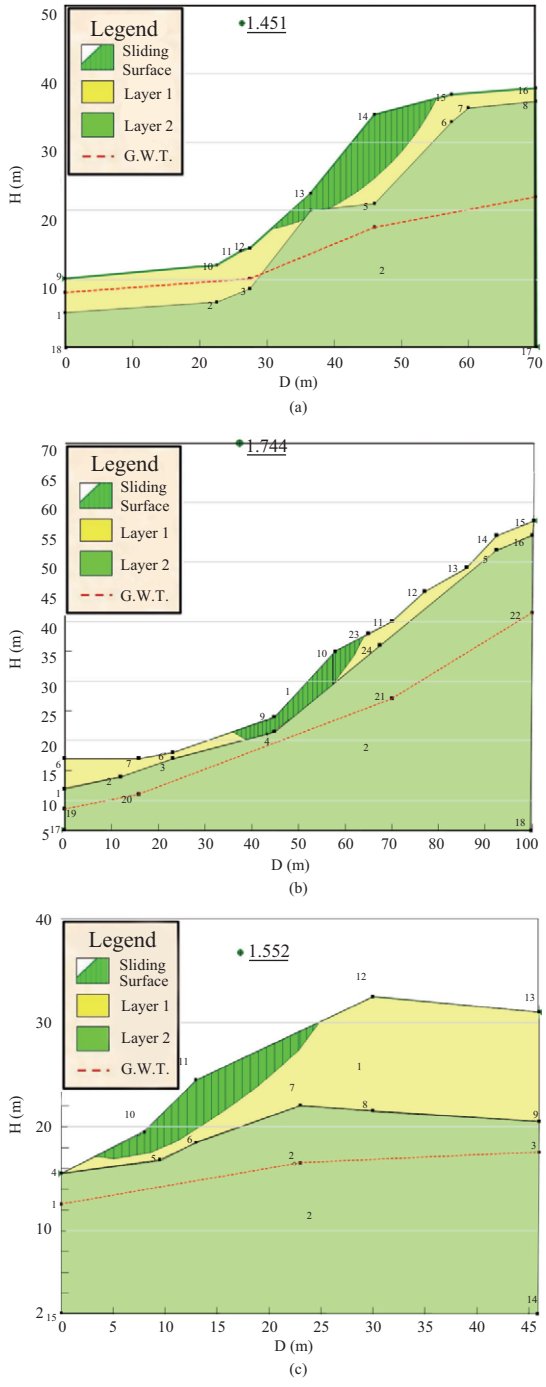

Fig. 5. (a) Slope stability results under normal conditions at L1-L1; (b) Slope stability results under normal conditions at L2-L2; (c) Slope stability results under normal conditions at L3-L3.

factor are as follows: L1-L1 = 1.451, L2-L2 = 1.744, L3-L3 = 1.552. These values reveal that the values for slope safety factor under normal conditions were within a safe range.

2) Typhoon Rainfall Conditions

The study area is located in the foothills of western Taiwan. Outcrop and drilling data revealed that nearby hills are composed of the Miocene, i.e., a Nanchuang layer and a gravel layer. A thick layer of massive sandstone makes up most of the layers.

Geometric models

In seeking to simulate actual conditions, we simplified the soil strata in the region into backfill, overburden layer, laterite gravel, moderate to highly weathered bedrock, weak weathered to fresh bedrock and other layers, as indicated in the real-time data. Setting boundary conditions for geometric models is an important step in constructing numerical simulations. Symbols used in Figs. 7-9 on the program interface are as follows: infiltration boundaries (·), impermeable boundaries in cases without seepage (when total seepage equals zero) (▲), seepage outlet boundaries (△).

Input parameters of material modes

Input parameters for seepage analysis

Two-dimensional transient flow conditions were adopted for seepage analysis. The input parameters used for seepage analysis are described in the following:

(1) Volumetric Water Content

In this study, we assumed the following values for saturated volumetric water content: backfill and overburden layer (0.35), laterite gravel layer (0.3), moderate to highly weathered bedrock (0.25), and bedrock (weak weathered to fresh) (0.21). These values were adopted from the results of Fredlund (1994).

(2) Hydraulic Conductivity Function

During rainfall, soil above the groundwater level may remain unsaturated, which means that hydraulic conductivity would vary with the saturation of the soil. Thus, the hydraulic conductivity function is a non-constant value and a function of time. To ensure consistency with real-time infiltration conditions, we adopted the hydraulic conductivity function as an input parameter. Even after conduction experiments on permeability, we were unable to determine the permeability coefficient under negative pore-water pressure conditions. Thus, we selected soils from the 24 soil hydraulic conductivity functions proposed by previous scholars (listed on SEEP/W) with permeability coefficient K (under saturated conditions) similar to those of the soils in this study.

Based on soil parameters (e.g., porosity n and soil constituents), we selected a program with built-in values that most closely resembled the conditions of the current study. We also referred to the study by Liu (1990), which lists the permeability coefficient of the red soil layer as $4.93 \times 10\text{-}6 \sim 4.77 \times 10\text{-}5$ m/sec. Table 5 presents a summary of data related to the hydraulic conductivity functions used for seepage analysis.

(3) Rainfall

As outlined in Chapter 2 (Table 3), Typhoon Nari (2001) produced the highest total rainfall in a single hour and the highest rainfall intensity recorded at CKS rainfall station. Thus, we focused on the simulation of a specific rainfall scenario, Typhoon Nari, the output rainfall hydrograph of which in presented in Fig. 6.

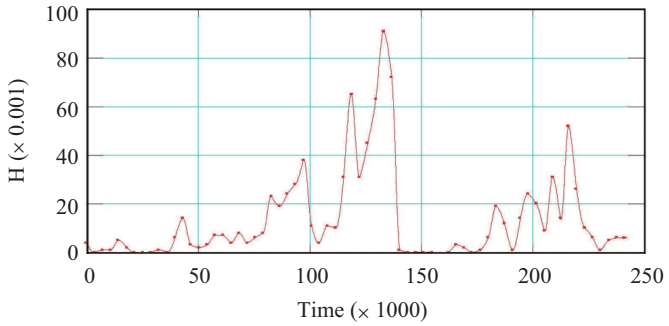

Fig. 6. Rainfall hydrograph of Typhoon Nari in 2001 converted to H (t) ~ t curve (Unit: sec-m).

Table 5. Input parameters: Hydraulic conductivity coefficient used for rainfall seepage analysis.

Geological conditions	Permeability coefficient K (m/sec)		
	Max. K_b	Mid. K_m	Min. K_s
Overburden layer and backfill	4.30×10^{-5}	1.40×10^{-7}	1.50×10^{-8}
Laterite gravel layer	4.77×10^{-5}	5.83×10^{-6}	4.93×10^{-6}
Moderate to highly weathered rock	2.50×10^{-7}	5.80×10^{-8}	1.50×10^{-8}
Weak weathered to fresh bedrock	5.80×10^{-8}	8.40×10^{-9}	1.00×10^{-9}

where K_b = maximum permeability coefficient, K_m = median permeability coefficient and K_s = minimum permeability coefficient.

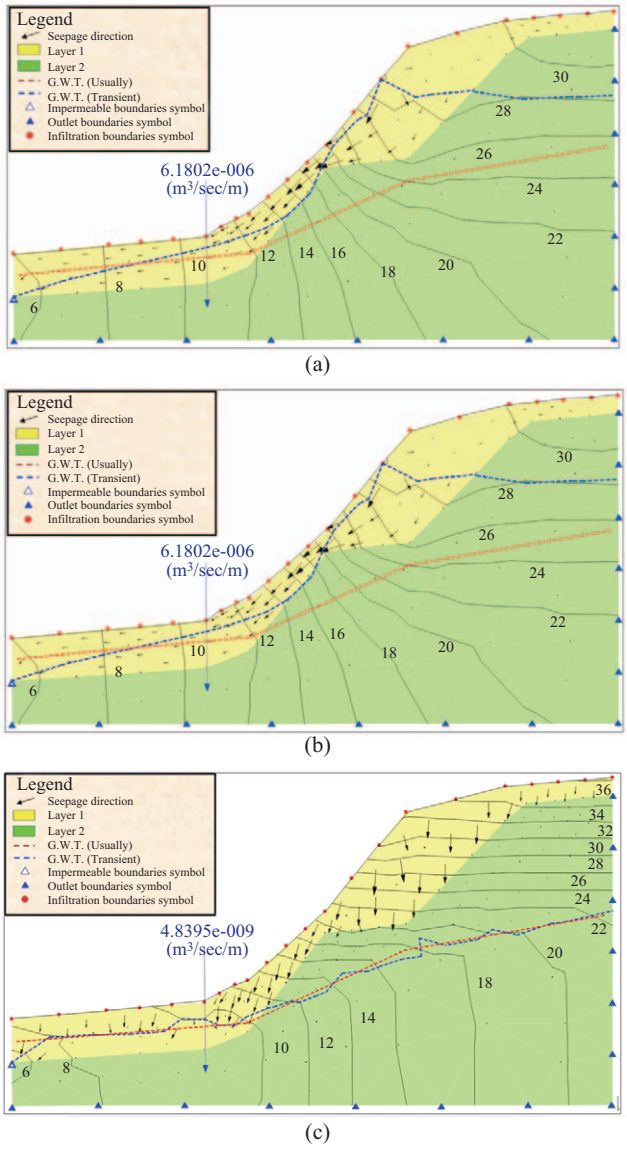

Fig. 7. Changes in groundwater levels on Time-step #6 in Section L1-L1 as determined by SEEP/W analysis: (a) $K_{1b} = 4.3 \times 10^{-6}$, $K_{2b} = 5.8 \times 10^{-8}$ (m/sec); (b) $K_{1m} = 1.4 \times 10^{-7}$, $K_{2m} = 8.4 \times 10^{-9}$ (m/sec); (c) $K_{1s} = 1.5 \times 10^{-8}$, $K_{2s} = 1.0 \times 10^{-9}$ (m/sec).

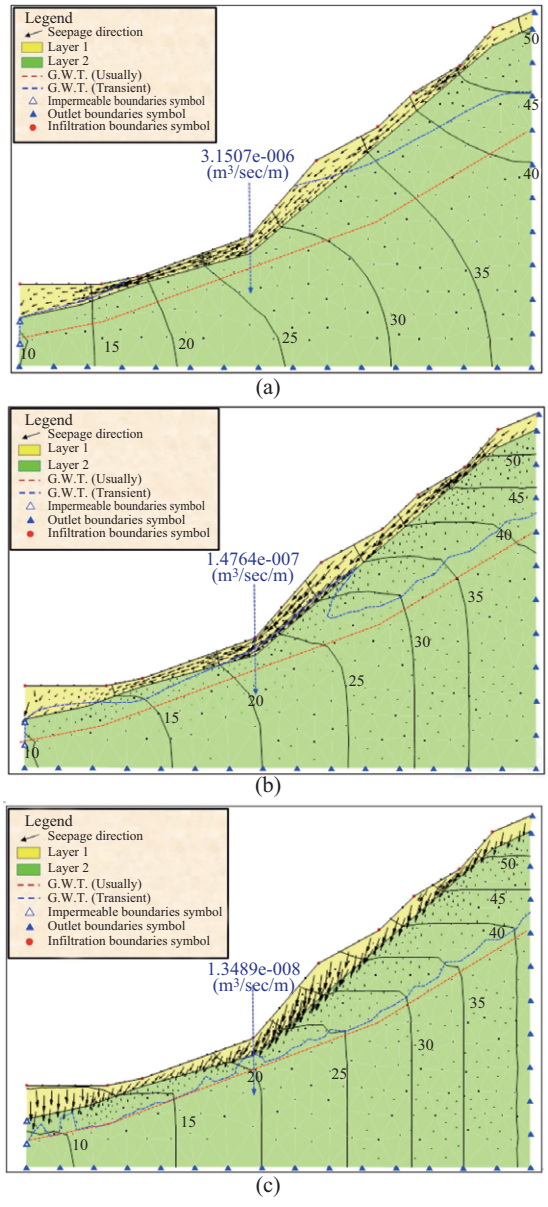

Fig. 8. Changes in groundwater levels on Time-step #6 in Section L2-L2 as determined by SEEP/W analysis: (a) $K_{1b} = 4.3 \times 10^{-6}$, $K_{2b} = 5.8 \times 10^{-8}$ (m/sec); (b) $K_{1m} = 1.4 \times 10^{-7}$, $K_{2m} = 8.4 \times 10^{-9}$ (m/sec); (c) $K_{1s} = 1.5 \times 10^{-8}$, $K_{2s} = 1.0 \times 10^{-9}$ (m/sec).

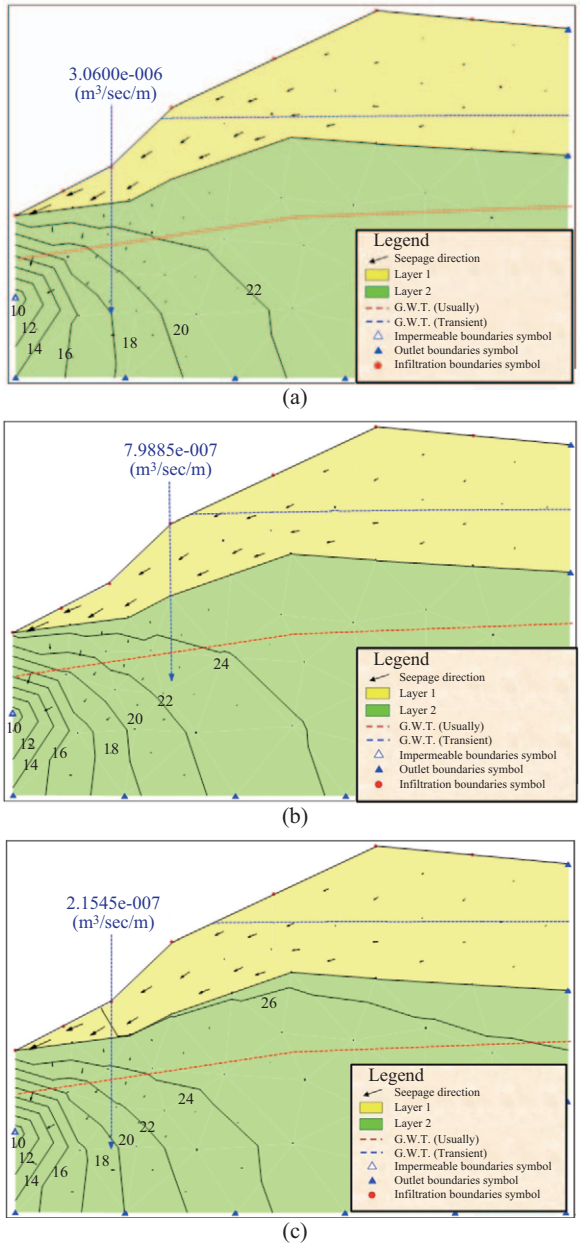

Fig. 9. Changes in groundwater levels on Time-step #6 in Section L3-L3 as determined by SEEP/W analysis: (a) $K_{1b} = 4.77 \times 10^{-5}$, $K_{2b} = 2.5 \times 10^{-7}$ (m/sec); (b) $K_{1m} = 4.93 \times 10^{-6}$, $K_{2m} = 1.5 \times 10^{-8}$ (m/sec); (c) $K_{1s} = 5.83 \times 10^{-6}$, $K_{2s} = 5.8 \times 10^{-8}$ (m/sec).

Rainfall infiltration

The amount of rainfall that infiltrates the slope depends on rainfall patterns, the permeability of the soil, and soil status prior to rainfall. Before initiating SEEP/W analysis, we entered the analytical conditions and related parameters into a finite element model, and then proceeded with analysis under a variety of rainfall durations. This study adopted a two-dimensional transient seepage model to analyze overall rainfall infiltration. SEEP/W provides pressure heads and water levels with increments of time used in a rainfall hydrograph.

Table 6. Setting of Time Step in this study.

Time Step	From the beginning time (hr)	Time Step	From the beginning time (hr)
1	1	11	96
2	2	12	104
3	4	13	112
4	8	14	120
5	16	15	128
6	32	16	136
7	64	17	144
8	72	18	152
9	80	19	160
10	88	20	168

Seepage and slope stability

This study used pressure head and pore-water pressure as input data for SLOPE/W in slope stability analysis. We also adopted methods proposed by Ordinary, Bishop, Janbu and Morgenstern-Price to perform calculations related to slope stability. Automatic positioning (Auto-Locate) can be used for sliding surfaces and manual setting are also available. Groundwater levels associated with the seepage of rain water varies according to the rate and duration of rainfall. We input SEEP/W data into SLOPE/W for analysis of slope stability, the results of which indicate that slope stability varies with the water level, which is a non-constant value FS (t).

To consider the influence of the typhoon-associated rainfall, this study employed transient analysis. SEEP/W analysis was divided into 20 time steps, as shown in the following Table 6 Rising groundwater levels are usually less obvious in the initial stages of a typhoon. Thus, rising groundwater levels resulting from surface infiltration in later periods or even after the typhoon should also be taken into account to ensure consistency with the actual events. Thus, we set the duration for infiltration analysis at 7 days (168 hours).

IV. DISCUSSION

1. Verification of Seepage Analysis Results

The hydraulic conductivity of saturated soils was divided into three sectional profiles with two layers for each profile (L1-L1, L2-L2 & L3-L3) for slope seepage analysis. Groundwater levels change with the rate and duration of rainfall; therefore, to facilitate further comparisons, we set the time point in a later stage of the typhoon as an initial condition for further analysis (Time step 6: between hour 32 and hour 64, the average rainfall intensity was between 20 mm/hr and 91 mm/hr). The results of slope seepage discharge are presented in L1-L1~L3-L3 in Fig. 7.

As shown in Figs. 7 and 8, in the case of low soil permeability (k <1 × 10-6 m/sec), the point of greatest permeability is concurrent with the highest groundwater level (up to about 10m). In addition to Figs. 7-9, where the blue dashed lines are

Table 7. Comparison of seepage discharge (Q) associated with Typhoon Nari in 2001 (time-step #6).

Section / Q (m^3/sec/m) / K (m/sec)	L1-L1	L2-L2	L3-L3
K_b	6.1802e-006	3.1507e-006	3.0600e-006
K_m	6.5002e-008	1.4764e-007	7.9885e-007
K_s	4.8395e-009	1.3489e-008	2.1545e-007

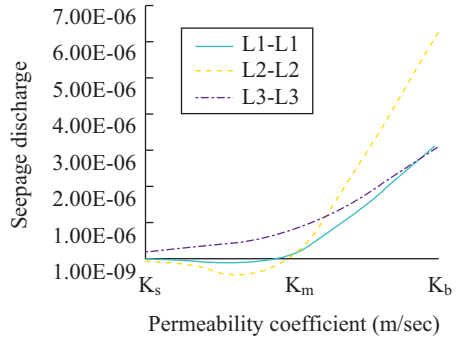

Fig. 10. Comparison of seepage discharge and permeability coefficient in section Sections L1~L3 (Time-step #6).

the groundwater level in time-step 6 of rainfall infiltration, and the red dashed lines line is the groundwater level in daily. Likewise, a reduction in the permeability coefficient is accompanied by a drop in groundwater levels (by as much as 4 m). When the permeability coefficient drops to its lowest value, the average groundwater level does not present significant uplift (1 m or less); therefore the water level is proportional to the coefficient of permeability.

Previous groundwater monitoring reports have indicated that groundwater levels in the elevated terrain are approximately 2.9 m to 3.3 m below the surface. On September 12, 2004, Tropical Storm Haima and the accompanying southwesterly airstreams caused the groundwater to gush out from the ground, and according to the calculations obtained in this study, the groundwater levels rose by approximately 4 m during Typhoon Nari. Comparisons with the onsite groundwater level observations show that the reliability of the results from this model is high.

In cases of high soil permeability, such as for the laterite gravel in Fig. 9 rapid infiltration means that the rise in water level is not necessarily faster than the drawdown speed. The assertions made in the preceding discussion are not necessarily supportable; therefore, we need to consider additional factors in order to obtain a conclusion. When the permeability coefficient is small, water infiltration tends to proceed vertically and when the permeability coefficient exceeds the saturated hydraulic conductivity of the soil, underground seepage tends to flow to lower slopes. Thus, the simulation and analysis results of SEEP/W are consistent with the general mechanical principles associated with soil.

Table 8. Moment equilibrium conditions in slope stability analysis (satisfying the limit equilibrium theory).

Analysis Method	Force-Equilibrium		Moment Equilibrium	FS
	X-direction	Y-direction		
Ordinary	No	No	Yes	Lowest
Bishop's simplified	Yes	No	Yes	2nd highest
Janbu	Yes	Yes	No	2nd lowest
Morgenstern-Price	Yes	Yes	Yes	Highest

Table 7 shows the corresponding seepage discharge values for each section, after adjusting the permeability coefficient. A comparison of seepage discharge and permeability coefficients is presented in Fig. 10. As shown in Table 7 and Fig. 10, the permeability coefficient is proportional to seepage discharge, which means that an increase in the permeability coefficient leads to a relative increase in slope seepage discharge.

2. Results of Slope Stability Analysis

1) Rainfall Duration and Slope Stability

This study used the medium of the permeability coefficients in Table 5 to explore the influence of rainfall duration on slope stability. In slope stability analysis, the safety factor was obtained from a variety of slicing methods: Ordinary, Bishop, Janbu, and Morgenstern-Price methods. Table 8 presents the conditions considered in the mechanical analysis of the slices.

The results of these four analysis methods demonstrate that the Ordinary method produces FSs that are smaller than those from the other three methods, regardless of the conditions. This is because the Ordinary method does not consider the lateral forces applied to the slices, such that the results are more reserved. Thus, we used the results of the Morgenstern-Price method in subsequent analysis.

In accordance with the change curve of time-steps in Fig. 11, it is clear that time steps 6 and 5 are the turning points of FS. This can be explained by the fact that infiltration continues during the late rainfall period of a typhoon, such that the safety factor continues to change. The overburden layer in Section L2-L2 is the shallowest; therefore, the saturation status of the soil and the safety factor continue dropping. In Section L1-L1, an increase in infiltration depth following the typhoon tended to raise the safety factor more slowly than that observed in the late period of the typhoon. Clearly, with the progress of time, rainfall infiltration becomes increasingly important to slope stability. These findings are consistent with the historical records of most typhoons in which disasters tend not to occur at the beginning of the event. Rather, landslides or debris flow generally occur in the later stages of a typhoon or even a day or two after the typhoon has passed.

In Section L3-L3, most of the safety factor values are less than 1.0 and therefore do not warrant consideration. Slope instability is probably caused by severely weathered bedrock. The extremely thick overburden layer (laterite gravel) has

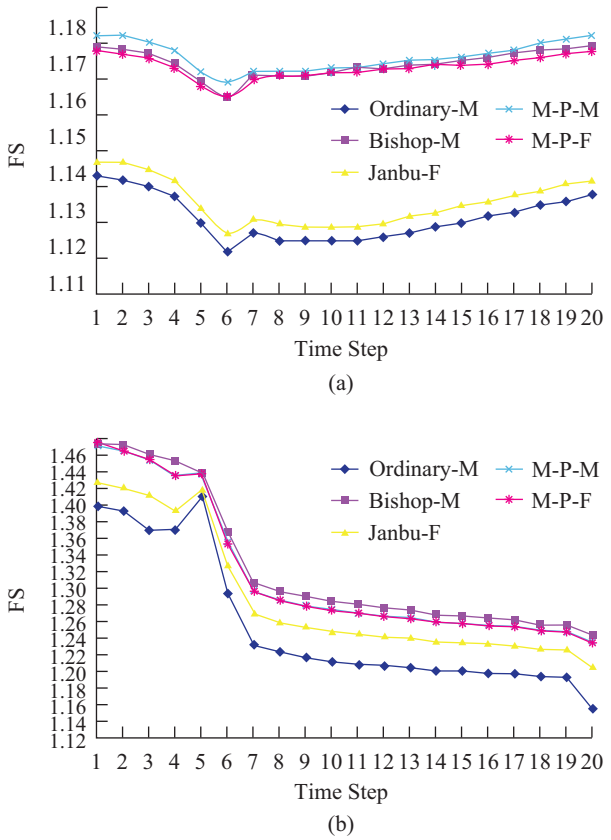

Fig. 11. Influence diagrams of time-step and safety factor following infiltration of rainfall from Typhoon Nari: (a) section L1-L1 and (b) section L2-L2.

permeability far higher than that found in other areas; therefore, simulation results of this block produced a rapid rise in groundwater levels following the typhoon, which produced a slope safety factor of less than 1.0.

2) Comparison with STABL and GEOSTUDIO Program

The previous Chang (2008) used the program STABL (using the Ordinary Sliced Method) to simulate the rising water level upon the approach of Typhoon Nari in the same study area of us. First, to facilitate a comparison of the conditions used in the two studies, we summarized the input parameters in Table 9. This enabled a preliminary comparison prior to analysis and discussion of the results. The content of the table shows that the settings of the STABL program are too simple; i.e., they lack many important parameters, such as the material parameter, K, and the simulated groundwater level during typhoons, as well as boundary conditions. These overly simple settings would preclude the use of these analysis results in simulating transient seepage during typhoons, thereby greatly undermining the accuracy of the FS simulation results. Secondly, Table 10 compares the relevant safety factors (FS) derived by Chang (2008) with those of this study. The results in Table 10 show that during normal rainfall conditions (i.e., no typhoons), the two programs present similar results (dif fering by less than

Table 9. Comparison of input conditions for GEOSTUDIO and STABL.

Item \ Researcher			Chang (2008)	This study	note
Analysis Program			STABL	GEOSTUDIO	
Input Parameter	Soil Parameter		Table 4	Table 4	γ_t, γ_{sat}, c', φ'
	Material Parameter		Permeability coefficient: Mein & Larson (1973) $K_s = 10^{-3}$ cm/sec (36 mm/hr): $1 > K_s$	1.Volumetric Water Content Function 2. Hydraulic Conductivity Function: Table 5	
Initial Condition (I.C.)	Typhoon period	Railfall pattern	Using rainfall of total average value and maximum in one field	The same	
		G.W.L.	Calculation of rainfall infiltration depth and groundwater recharge coefficient: 1. Total average value: 2.26 m × 36% = 0.81 m (Conservative assumption that the groundwater level rises by 1 m) 2. Maximum in one field: 9.5 m × 36% = 3.42 m (Conservative assumption that the groundwater level rises by 4 m)	Input the rainfall diagram of Typhoon Nari into SEEP/W program, then we can get the rainfall hyetograph (Fig. 6)	
Boundary Condition (B.C.)			Only the positions of the soil interface can be input	In addition to the positions of the soil interface, the boundary symbol conditions can be set (▲, △, ·)	
LEM			Carter's Method	SLOPE/W: Ordinary Method	
Considering the changes of the pore-water pressure			No	Yes	

10 %). However, excluding Section L3-L3, the failure of which has already been explained in the previous section, the FS values in the event of extreme rainfall are all less than those derived by Chang (2008). This is likely due to the fact that STABL uses static water levels to analyze pore-water pressure, whereas SEEP/W uses transient rainfall seepage. Thus, the inclusion of seepage leads to smaller FS values. Another reason for these large differences may be the different slicing methods that were employed. However, these results show that the FS of Section L3-L3 barely changes, which is not a normal occurrence. We can therefore infer that when STABL is used to analyze typhoon-induced rainfall, the resulting FS values are on the high side, which can easily lead to an overestimation regarding the actual danger of slopes.

Table 10. Comparison of safety factors associated with slope stability in various sections of the study area.

Item \ Researcher				Chang (2008)	This study	Comparison
Analysis Program				STABL	GEOSTUDIO	Differences
FS	Typical		L1-L1	1.50	1.451	3.38%
			L2-L2	1.94	1.744	11.24%
			L3-L3	1.53	1.552	-1.42%
	Typhoon Rainfall	1 m GWT. Uplift (Beginning)	L1-L1	1.50	1.120	33.93%
			L2-L2	1.94	1.391	39.47%
			L3-L3	1.53	0.602	154.15%
		4 m GWT. Uplift (End)	L1-L1	1.38	1.115	23.77%
			L2-L2	1.94	1.202	61.40%
			L3-L3	1.52	0.352	331.82%

3) Future Considerations in Engineering Design

To maintain a degree of safety, the FS values of engineering designs are generally greater than 1.0. As for what counts as reasonable, two factors can be taken into consideration:

(1) A grasp of geological and groundwater conditions as well as the strength of the strata; or a full comprehension of uncertain factors;
(2) The importance of the slope's location (in other words, the severity of the damage that would be incurred in the event of a slope failure).

A reasonable FS can be determined from the two perspectives above. As for actual engineering design, the authors of the Development and Building Bases on Hillsides in Taipei City: Technical Planning and Design Specifications suggest the following conservative FS standards: (1) normal circumstances: F.S. = 1.5; (2) storms: F.S. = 1.2; (3) earthquakes: F.S. = 1.1.

Based on these standards, we can see that the FS values of Section L3-L3 are less than 1.0. The planning of large-scale building in this area should thus be avoided. If it cannot be avoided, then the stability of the slope must be enhanced through artificial means. In contrast, the FS values of Section L1-L1 are all greater than 1.1, thus only simple measures would be required to enhance drainage on the slope in order to increase the FS. As for Section L2-L2, the FS values are all around 1.2; therefore, maintaining the status quo should be sufficient.

The community in the study area comprises high-grade residences; therefore, comprehensive monitoring data is available. Nonetheless, it is sensitive and difficult to obtain by outsiders. We suggest that the management of the study area use the rainfall partition approach developed in this study and the relationship between groundwater level increases and rainfall duration with regard different rainfall types (such as the extreme rainfall events during Typhoon Xangsane in 2000, Typhoon Nari in 2001, Typhoon Sinlaku in 2008, and Typhoon Saola in 2012) to develop the local empirical equations by regression analysis. We also suggest the management office of this community to use the empirical equations along with the up to date groundwater level monitoring and reporting system to achieve the effect of slope disaster alarm. When the levels approach the safety limit (By using the develop regression equations), they should keep close watch over the drainage of the retaining wall in case the water pressure in the slope cannot be released, which could cause slope instability. The use of these groundwater data should make it easy to establish a simple alarm for disaster prevention.

4) Impact Analysis of Numerical Modeling Parameters

The high rainfall intensity of storms causes a rapid increase in surface saturation due to the accumulation of rainwater. The soil immediately forms an "infiltration zone", which decreases the shear strength of the slope. The slope located at top of the normal water level is unsaturated for a long period of time; therefore, the infiltration of water from heavy rains breaks the existing matric suction of the slope, resulting in the formation of a "Wetting Band", which reduces the shear strength of the soil. This is the main reason for shallow failure on unsaturated slopes.

Taking samples (in situ) without disturbing the soil can be exceedingly difficult; therefore, the values c' and φ' of shear strength must be obtained by triaxial tests or direct shear tests performed in a laboratory. This study adopted the concept of c' reduction to conduct safety factor analysis during slope stability analysis. This process involves gradually reducing the shear strength and observing the critical point at which damage occurs.

As shown in Fig. 12, reducing c has no more effect on FS than does a reduction in φ'. The shallow soil undergoes failure most rapidly after being soaked with water. However, φ' is difficult to analyze because it has been reduced too much; therefore, we discuss only the value of c', the changes of which are linear. Every reduction of 10 % leads to a 3.5% reduction in the FS value.

V. CONCLUSIONS

This study collected rainfall data associated with typhoons that struck northern Taiwan over the last 17 years. We adopted the intensely developed hillsides in Xindian, close to Taipei City, as the area of study. We developed a rain-field division method to facilitate the selection of the most representative rainfall event (Typhoon Nari in 2001) to provide input data for the finite-element analytical software SEEP/W. We then performed two-dimensional transient seepage analysis of unsaturated soil and entered the PWP results into subprogram SLOPE/W to conduct analysis on slope stability. It is hoped that this pre-development slope stability analysis will prove valuable in future planning and design. In the following, we present various conclusions and suggestions from this analysis.

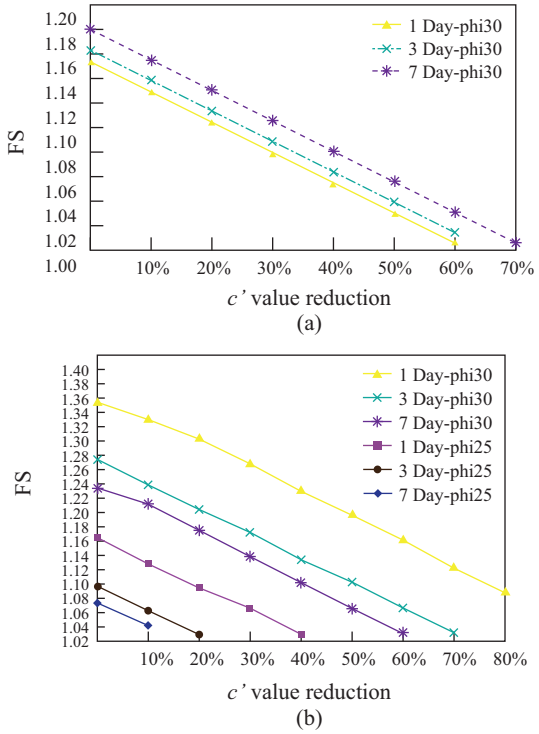

Fig. 12. Trend of reduction in c' value and safety factor: (a) section L1-L1 and (b) section L2-L2.

(1) Among the 35 typhoons that struck northern Taiwan, the peak in the third quarter section accounted for 31% of the total rainfall and typhoon Nari presented the highest rainfall intensity about of 13.5 mm/hr in a field , and maximum to 91 mm/hr in an hour. This indicates that the highest rainfall is likely to occur in the later stages of the typhoon and the highest rainfall in a single field and within a single hour occurred in the same typhoon.

(2) Analysis results show that the point of greatest permeability is concurrent with the highest groundwater level (up to about 10 m). Likewise, a reduction in the permeability coefficient is accompanied by a drop in groundwater levels (by as much as 4 m). When the permeability coefficient drop to its lowest value, the average groundwater level does not present significant uplift (less than 1m). Thus, we can infer that the groundwater level is proportional to permeability coefficient.
When the permeability coefficient is small, infiltration water tends to flow vertically. When permeability exceeds the saturated hydraulic conductivity of the soil, underground seepage flows to lower areas.

(3) Section L3-L3 in the study area was identified as an unsafe slope, according to rainfall infiltration and slope stability analysis. This can be explained by the following two points: (i) the highest rainfall intensity (for 1 hour) during Typhoon Nari was 91 mm/hr. According to Brand et al. (1984), the threshold value for slope failure is 70 mm/hr. (ii) This slope has undergone more pronounced weathering than have the other two locations. In addition, the laterite gravel layer in this area has high permeability and the thickest overburden. Suitable drainage must be installed before the development of the region in order to avoid slope disasters in the future. Improvements in the condition of soil should be conducted before endeavoring to build on this area.

(4) We employed the shear angle φ' of the shear strength and the effective cohesion c' reduction to simulate slope failures in the shallow layer following typhoon-induced saturation with rain water. A reduction in φ' was shown to have a more pronounced impact on FS values than did a reduction in c'. The geological conditions in the study revealed that in this case, φ' is the main controlling parameter associated with the safety factor. However, φ' is difficult to analyze because it has been reduced too much; therefore, we discuss only the value of c', the changes of which are linear. Every reduction of 10 % leads to a 3.5% reduction in the FS value.

(5) To summarize, the rainfall type-rain-field division model proposed by Jan et al. (2003) and Lee (2006) in this study can be used in conjunction with rainfall hydrographs from SEEP/W to simulate two-dimensional transient seepage in the soil. SLOPE/W results (the relationship between rainfall duration and pressure head) could provide FS values of slope stability. In contrast, the more commonly used STABL employs a simple calculation method to simulate the rise in groundwater levels associated with rainfall intensity and considers only static water levels in pore-water pressure analysis. It does not fully take into account the dynamic seepage caused by extreme rainfall. Comparison with the achievements of this study under the same conditions revealed that the FS values obtained using STABL are relatively higher, which can easily lead to misjudgments in the assessment of dangerous slopes. The more comprehensive evaluation model developed in this study is able to more accurately describe transient seepage in the study area under the influence of extreme rainfall.

(6) In the practical application of engineering, the model developed in this study can be used to assess the feasibility of measures to protect the slopes in similar areas of northern Taiwan, thereby preventing excessive construction on artificial slopes. Similarly, in areas with developed slopes, a simple local warning system could be established using increases in groundwater levels to process groundwater monitoring data for disaster prevention.

NOTATIONS

The following symbols are used in this paper:

C = the change in volumetric water content per unit change in pressure head
c' = effective cohesion
FS = factor of safety
K = permeability coefficient

K_b = maximum permeability coefficient
K_m = medium permeability coefficient
K_s = minimum permeability coefficient
PWP = Pore-water Pressure
φ' = effective friction angle
γ_{sat} = unit weight of saturated soil
γ_t = unit weight of moist soil
▲ = impermeable boundaries symbol in SEEP/W program
△ = seepage outlet boundaries symbol in SEEP/W program
• = infiltration boundaries symbol in SEEP/W program

REFERENCES

Aleotti, P. A. (2004). Warning system for rainfall-induced shallow failures. Engineering Geology, 73(3-4), 247-265.

Bonnard, Ch. and F. Noverraz (2001). Influence of climate change on large landslides: assessment of long term movements and trends. Proc. of the International Conference on Landslides: causes impact and countermeasures, Gluckauf, Essen, Davos, 121-138.

Brand, E. W. (1982). Analysis and design in residual soil. In Proceedings of the ASCE Geotechnical Engineering Division Specialty Conference Engineering and Construction in Tropical and Residual Soils, Honolulu, Hawaii, 89-141.

Brand, E. W., J. Permchitt and H. B. Phillipson (1984). Relationship between rainfall and landslides in Hong Kong. Proceedings 4th international symposium on landslides, Vol. 1, Toronto, Canada, 377-384.

Caine, N. (1980). The rainfall intensity duration control of shallow landslides and debris flows. Geogr. Ann. 62 (1-2), 23-27.

Campbell, R. H. (1975). Debris flow originating from soil slip during rainstorm in southern California. Q. Enginerring Geologist 7, 339-349.

Cannon, S. H. and S. D. Ellen (1985). Rainfall conditions for abundant debris avalanches, San Francisco Bay region, California. California Geology 38(12), 267-272.

Cannon, S. H. (1988). Regional rainfall-threshold conditions for abundant debris-flow activity. In: Ellen, S. D. and G. F. Wieczorek (Eds.), Landslides, Floods and Marine Effects of the Storm, San Francisco Bay Region, California, 35-42. USGS Prof. Paper 1434.

Chang, S.-Y. (1995). The Research of Rainfall Division Events. Agricultural Engineering. (in Chinese)

Chang, R.-C. (2004). Xindian City of Taipei County Scenic Base - Analysis Report of Additional Investigations of Hillside Engineering Geology Environment. for J. C. Chang Consulting Engineering Ceologist, Inc., Taipei, Taiwan, Republic of China. (in Chinese)

Chang, D.-F. (2008). The study of typhoon induced rainfall on the analysis of slope stability. Master's Thesis, Department of Harbor and River Engineering, National Taiwan Ocean University, Taiwan, Republic of China, unpublished. (in Chinese)

Corominas, J. and J. Moya (1999). Reconstructing recent landslide activity in relation to rainfall in the Llobregat river basin, Eastern Pyrenees, Spain. Geomorphology 30, 79-93.

Crosta, G. (1998). Regionalization of rainfall thresholds: an aid to landslide hazard evaluation. Environmental Geology 35 (2-3), 131-145

Crozier, M. J. and T. Glade (1999). Frequency and magnitude of landsliding: fundamental research issues. Zeitschrift fur Geomorphologie N. F. 15, 141-155.

Dahal, R. K., S. Hasegawa, M. Yamanaka, S. Dhakal, N. P. Bhandary and R. Yatabe (2009). Comparative analysis of contributing parameters for rainfall-triggered landslides in the Lesser Himalaya of Nepal. Environmental Geology 58(3), 567-586.

Flentje, P., R. N. Chowdhury and P. Tobin (2000). Management of landslides triggered by a major storm event in Wollongong, Australia. Proc. of the II International Conference on Debris-Flow Hazards Mitigation, Mechanics, Prediction and Assessment, Taipei, 479-487.

Fredlund, D. G. and A. Xing (1994). Equations for The Soil-Water Characteristic Curve, Canadian Geotechnical Journal 31, 521-532.

Geo-Slope International Ltd. (2004). SEEP/W of GEO-SLOPE OFFICE for Finite Element Seepage Analysis, User's Guide. The United States.

Geo-Slope International Ltd. (2004). SLOPE/W of GEO-SLOPE OFFICE for Slope Stability Analysis, User's Guide. The United States.

Guzzetti, F., G. Crosta, M. Marchetti and P. Reichenbach (1992). Debris flows triggered by the July, 17-19, 1987 storm in the Valtellina Area (Northern Italy). Proc. of the VII International Congress Interpraevent, Bern 2, 193-204.

Hsu, M.-L. and Z.-C. Huang (2000). Simulation of unsaturated infiltration layer in one-dimensional. In Conference on Computer Applications in Civil and Hydraulic Engineering, Taiwan, 2101-2110. (in Chinese)

Jan, C.-D., M.-H. Lee and T.-H. Huang (2003). Effect of rainfall on debris flows in central Taiwan. International Conference on Slope Engineering, Hong Kong, 751-756.

Lee, L.-M., N. Gofar and H. Rahardjo (2009). A simple model for preliminary evaluation of rainfall-induced slope instability. Engineering Geology 108 (3-4), 272-285.

Lee, M.-H. (2006). A rainfall-based debris-flow warning analysis and its application. Ph.D. Thesis, Department of Hydraulic and Ocean Engineering, National Cheng Kung University, Tainan, Taiwan, Republic of China, unpublished. (in Chinese)

Liu, J.-N. (1990). A comprehensive study of slope landslides in laterite plateau. Master's Thesis, National Taiwan University, Taipei, Taiwan, Republic of China, unpublished. (in Chinese)

Lui, M.-J. (2004). Discussion of Rainfall Infiltration Behavior of Soil Slope. Master's Thesis, Chung Yuan University, Taoyuan, Taiwan, Republic of China, unpublished. (in Chinese)

Lumb, P. (1975). Slope failures in Hong Kong. Quarterly Journal Engineering Geology 8, 31-65.

Montgomery, D. R. and W. E. Dietrich (1994). A physically-based model for the topographic control on shallow landsliding. Water Resources Research 30, 1153-1171.

Morgan, B. A., G. F. Wieczorek, R. H. Campbell and P. L. Gori (1997). Debris flow hazards in areas affected by the June 27, 1995 storm in Madison County, Virginia. USGS Open File Report, 97-438.

Paronuzzi, P., M. Del Fabbro and P. Maddaleni (2002). Frane superficiali tipo slide debris flow causate dal nubifragio del 21/22 giugno 1996 nella Val Chiarso` (Alpi Carniche, Friuli). Memorie della Societa Geologica Italiana 57, 443-452. (in Italian)

Shih, D.-S. (2001). The study of pattern analysis of typhoon rainfall in Taiwan area. Master's thesis, Department of Civil Engineering, National Central University, Chung-Li, Taiwan, Republic of China. (in Chinese)

Slosson, J. E. (1969). The role of engineering geology in urban planning. In: The Governor's conference on environmental geology. Colorado geological survey special publication 1, Denver, The United States, 8-15.

Slosson, J. E. and J. P. Krohn (1982). Southern California landslides of 1979 and 1980. In: Storms, floods, and debris flows in Southern California and Arizona, 1978 and 1980. Proceedings of symposium, national research council and environmental quality laboratory, California Institute of Technology, Pasadena. National Academy Press, Washington, D.C., 291-319.

Slosson, J. E. and R. A. Larson (1995). Slope failures in southern California: Rainfall threshold, prediction, and human causes. Environmental & Engineering Geo-Science 1(4), 393-401.

Taipei City Government (1989). Development and Building Bases on Hillsides in Taipei City: Technical Planning and Design Specifications, Taipei, Taiwan, Republic of China. (in Chinese)

Central Weather Bureau (2013). Website of Typhoon database, Accessed June 1. http://rdc28.cwb.gov.tw/.

Terlien, M. T. J. (1998). The determination of statistical and deterministic hydrological landslide-triggering thresholds. Environmental Geology 35(2-3), 125-130.

Water Resources Planning Institute, Water Resources Agency, Ministry of Economic Affairs (2012). A Study of Flood control and Sediment Management due to Climate Change of Tamsui River (1/2), Taipei, Taiwan, Republic of China. (in Chinese)

Wieczorek, G. F. (1987). Effect of rainfall intensity and duration on debris

flows in central Santa Cruz Mountains, California. In: Costa, Wieczorek (Eds.), Debris Flows/Avalanches: Processes, Recognition and Mitigation. Reviews in Engineering Geology 7. Geological Society of America, 23-104.

Wilson, R. C., R. K. Mark and G. E. Barbato (1992). Operation of real-time warning system for debris flows in the San Francisco Bay area, California. In: Shen, H. W. and F. Wen (Eds.), Hydraulic Engineering '93. Proceedings of the 1993 Conference, Hydraulics Division 2. American Society of Civil Engineers, San Francisco, CA, 1908-1913.

Wilson, R. C. and G. F. Wieczorek (1995). Rainfall thresholds for the initiation of debris flow at La Honda, California. Environmental and Engineering Geoscience 1(1), 11-27.

Zhang, L.-L., D. G. Fredlund, L.-M. Zhang and W.-H. Tang (2004). Numerical study of soil conditions under which matric suction can be maintained. Canadian Geotechnical Journal 41(4), 569-582.